Cholinergic and serotonergic modulations differentially affect large-scale functional networks in the mouse brain.

Shah D, Blockx I, Keliris GA, Kara F, Jonckers E, Verhoye M, Van der Linden A.

Bio-Imaging Lab, University of Antwerp, Universiteitsplein 1, Wilrijk, 2610, Antwerp, Belgium

Corresponding author:
D Shah
disha.shah@uantwerpen.be

Published in: Brain Struct Funct. 2015 Jul 21.
Doi: 10.1007/s00429-015-1087-7

Title: **Cholinergic and serotonergic modulations differentially affect large-scale functional networks in the mouse brain**

Authors:

Disha Shah[1], Ines Blockx[1], Georgios A. Keliris[1,2], Firat Kara[1], Elisabeth Jonckers[1], Marleen Verhoye[1], Annemie Van der Linden[1]

Authors affiliations:

[1] Bio-Imaging Lab, University of Antwerp, Universiteitsplein 1, 2610 Wilrijk, Antwerp Belgium.

[2] Max Planck Institute for Biological Cybernetics, Spemannstrasse 38, 72076 Tuebingen, Germany

Corresponding author:

Disha Shah

Bio-Imaging Lab, University of Antwerp, Universiteitsplein 1, 2610 Wilrijk, Antwerp Belgium

email: Disha.Shah@uantwerpen.be

Phone: + 32 (0)3 265.27.62.

Keywords:

Cholinergic; serotonergic; functional connectivity; default-mode network; functional networks; mouse brain

Abstract

Resting-state functional MRI (rsfMRI) is a widely implemented technique used to investigate large-scale topology in the human brain during health and disease. Studies in mice provide additional advantages, including the possibility to flexibly modulate the brain by pharmacological or genetic manipulations in combination with high throughput functional connectivity (FC) investigations. Pharmacological modulations that target specific neurotransmitter systems, partly mimicking the effect of pathological events, could allow discriminating the effect of specific systems on functional network disruptions. The current study investigated the effect of cholinergic and serotonergic antagonists on large-scale brain networks in mice. The cholinergic system is involved in cognitive functions and is impaired in e.g. Alzheimer's disease, while the serotonergic system is involved in emotional and introspective functions and is impaired in e.g. Alzheimer's disease, depression and autism. Specific interest goes to the Default-Mode-Network (DMN), which is studied extensively in humans and is affected in many neurological disorders. The results show that both cholinergic and serotonergic antagonists impaired the mouse DMN-like network similarly, except that cholinergic modulation additionally affected the retrosplenial cortex. This suggests that both neurotransmitter systems are involved in maintaining integrity of FC within the DMN-like network in mice. Cholinergic and serotonergic modulations also affected other functional networks, however, serotonergic modulation affected the frontal and thalamus networks more extensively. In conclusion, this study demonstrates the utility of pharmacological rsfMRI in animal models to provide insights into the role of specific neurotransmitter systems on functional networks in neurological disorders.

1. Introduction

In resting-state functional Magnetic Resonance Imaging (rsfMRI), low frequency (0.01-0.1Hz) fluctuations of the blood-oxygenation-level-dependent (BOLD) signal are considered to reflect underlying fluctuations of neural activity. Functional connectivity (FC) is defined as the temporal correlation of BOLD-fluctuations between spatially distinct areas (Biswal et al., 1995). The greatest advantage of rsfMRI is the possibility to investigate large-scale functional networks in a non-invasive way. Several applications of rsfMRI in humans demonstrated the existence of resting-state brain networks in the healthy brain and how these networks are modulated during disease (Damoiseaux et al., 2006, Buckner et al., 2008, Buckner et al., 2009, Bullmore and Sporns, 2009, Lee et al., 2013, Rohrer and Rosen, 2013, Sheline and Raichle, 2013, Brier et al., 2014, Hannawi et al., 2015, Iwabuchi et al., 2015).

Although rsfMRI studies in humans have provided invaluable insight into how the brain is organized in functional networks, studies in healthy rodents and rodent models of human neurological disorders might offer more flexibility to investigate the effect of specific modulations on the functional organization of the brain. For example, our recent study showed how modulating the cholinergic system with a muscarinic cholinergic receptor (mAChR) antagonist and agonist affects specific memory-related functional connections in the mouse brain e.g. FC between the hippocampus and thalamus, between the cingulate and retrosplenial cortex, and between the visual and retrosplenial cortex (Shah et al., 2015). These FC alterations could be linked to changes in memory performance, consistent with the known involvement of mAChRs in cognitive processes. While these results demonstrated that cholinergic modulations affect FC in the mouse brain, the focus was on specific functional connections rather than entire functional networks. Investigating the effect of pharmacological modulations on the network level would provide knowledge on the functional organization of the healthy mouse brain, mimic how early-stage pathological events might affect functional networks and demonstrate whether this could be linked to the organization of healthy and diseased brain networks in humans. The latter is of specific interest, considering the existence of numerous interesting mouse models of human disorders.

The most extensively studied network in humans is the Default-Mode-Network (DMN), a large-scale brain network consisting of brain regions that show highly correlated brain activity during rest and reduced activation during attentionally demanding tasks. DMN activity seems to be associated with

learning, creativity, emotions and cognitive functions in humans (Buckner et al., 2008). Thus, it is not surprising that DMN FC is disrupted in many neurological disorders such as Alzheimer's disease (Sheline and Raichle, 2013), depression (Sheline et al., 2009), autism spectrum disorders (Washington et al., 2014) and schizophrenia (Salvador et al., 2010). A few recent studies demonstrated the existence of a brain network in rats (Lu et al., 2012) and mice (Sforazzini et al., 2014, Stafford et al., 2014) that is spatially similar to the human DMN. The rodent DMN-like network consists of the prelimbic cortex, orbitofrontal cortex, cingulate and retrosplenial cortex, parietal and temporal association cortex, hippocampus and parts of the thalamus. Establishing sound protocols for repeated observations of the DMN-like network in mice and pinning down its key neurotransmitter systems would be a major step forward in unraveling DMN dysfunctions in mouse models of neurological disorders.

The cholinergic and serotonergic systems are particularly interesting for a number of diseases affecting the brain at the network level, thereby disturbing the DMN and potentially other networks. Muscarinic cholinergic receptors (mAChR) are involved in cognitive functions such as learning and memory, and are located in the hippocampus, several cortical areas and the striatum, thus showing considerable functional and spatial overlap with the DMN (Levey et al., 1991). Aberrant functioning of the mAChRs, as occurs in Alzheimer's disease, might cause the known FC deficits on the network level, such as in the DMN and other cognitive networks, and result in cognitive dysfunctions (Sheline and Raichle, 2013). The serotonergic system is, similar to the cholinergic system, involved in memory processes through 5HT receptors in the frontal, cingulate and retrosplenial regions (Hahn et al., 2012). However, the highest 5HT receptor density is found in the frontal cortex (Fleming et al., 2010), and it is known that the serotonergic systems plays an important role in frontally mediated behaviors such as emotional behavior, attention and introspective processes (Roberts, 2011). Moreover, diseases where these aforementioned behaviors are impaired, such as depression, schizophrenia and autism, are associated with aberrant FC in frontal regions and the DMN (Broyd et al., 2009, Jeong et al., 2009, Monk et al., 2009, Veer et al., 2010). Specific dysfunctions in the serotonergic system might thus result in FC deficits not only in the DMN, but also in frontal and thalamic networks, causing changes in the interaction between cognitive processes and emotional behavior.

In the current study we performed acute pharmacological modulations of the mAChR and 5HT1A receptors and investigated whether these receptors are involved in maintaining FC of the DMN-like

network and other brain networks in mice. Furthermore, we compared the differences between functional connections affected by both these neuromodulators. Our working hypothesis was that mAChRs and 5HT1A modulations cause similar changes in FC of cognitive and attention networks but serotonergic modulation would have a greater influence in frontal networks, considering the importance of this neurotransmitter system in frontally-mediated behaviors.

2. Material and Methods

2.1. Ethical statement

All procedures were performed in strict accordance with the European Directive 2010/63/EU on the protection of animals used for scientific purposes. The protocols were approved by the Committee on Animal Care and Use at the University of Antwerp, Belgium (permit numbers 2012-48 and 2013-62) and all efforts were made to minimize animal suffering.

2.2. Animals

Male C57BL/6 mice of 12 weeks old were used throughout the entire study (Jax strain, Charles River Laboratories). For the handling procedures the mice were anesthetized with 2% isoflurane (IsoFlo, Abbott, Illinois, USA), which was administered in a mixture of 70% N2 and 30% O2. The physiological status of all animals was monitored throughout the MR imaging procedure. A pressure sensitive pad (MR-compatible Small Animal Monitoring and Gating system, SA Instruments, Inc.) was used to monitor breathing rate and a rectal thermistor with feedback controlled warm air circuitry (MR-compatible Small Animal Heating System, SA Instruments, Inc.) was used to maintain body temperature at (37.0 ± 0.5)°C. For the pharmacological MRI (phMRI) measurements all mice were anesthetized with 1.5% isoflurane. During the resting-state functional MRI (rsfMRI) measurements, medetomidine (Domitor, Pfizer, Karlsruhe, Germany) was used to sedate the animals (Jonckers et al., 2011, Shah et al., 2013) and was administered as a bolus injection of 0.3mg/kg. After the imaging procedures, the effects of medetomidine were counteracted by injection of 0.1mg/kg atipamezole (Antisedan, Pfizer, Karlsruhe, Germany).

PhMRI was performed to determine the pharmacodynamics of a single bolus of medetomidine (0.3mg/kg, s.c. catheter) in the mouse brain (N=10). Pharmacological rsfMRI was then performed to evaluate the effects of medetomidine, and cholinergic and serotonergic modulations on functional

connectivity (N=15/group). Two groups of healthy C57BL/6 mice were injected with medetomidine (0.3mg/kg, s.c.) and rsfMRI scans were acquired either at 20 min post-injection or at 50 min post-injection. Additionally, three groups of healthy C57BL/6 mice were injected with either saline (10ml/kg, s.c.), the mAChR antagonist scopolamine (3mg/kg, s.c.) (scopolamine hydrobromide trihydrate, Sigma Aldrich) or the serotonergic 5HT1A receptor antagonist WAY100135 (3mg/kg, s.c.) (WAY100135, Sigma Aldrich). Cholinergic inhibitors induce vasoconstriction which might affect neurovascular coupling and thus the BOLD-signal, especially considering the known overlap of the DMN-like network with major vessels (Dorr et al., 2007). Therefore, in order to investigate peripheral and neurovascular effects, we additionally evaluated FC changes induced by the peripherally acting mAchR antagonist methyl-scopolamine (3mg/kg, s.c.) (scopolamine methyl-bromide, Sigma Aldrich) and the 5HT1B/1D receptor agonist sumatriptan (10mg/kg, s.c.) (sumatriptan succinate, Sigma Aldrich) in two additional groups of mice. The injected volume was 0.3 ml for all groups. For each group, rsfMRI scans were acquired at 50 min after the injection of medetomidine, as at this time point the effect of medetomidine stabilized (cfr. results section). The doses were chosen based on behavior studies demonstrating at which doses behavior deficits could be observed in rodents. Furthermore, the same studies demonstrate that behavior deficits occur about 20 min (scopolamine, WAY100135, methyl-scopolamine) or 30 min (sumatriptan) after the injection of the respective compounds (Fletcher et al., 1993, Carli et al., 1995a, Carli et al., 1995b, Przegalinski et al., 1995, File et al., 1996, Ghelardini et al., 1996, Yu and Lewander, 1997, Schwarz et al., 1999, Carli et al., 2000, Ghelardini et al., 2009, Klinkenberg and Blokland, 2010). Therefore, rsfMRI scans were acquired 20 min after the injection of saline, scopolamine, WAY100135 and methyl-scopolamine, and 30 min after the injection of sumatriptan.

2.3. MRI procedures

MRI was performed on a 9.4T Biospec MRI system (Bruker BioSpin, Germany) with the Paravision 5.1 software (www.bruker.com). Images were acquired using a standard Bruker crosscoil set-up using a quadrature volume coil and a quadrature surface coil designed for mice. Three orthogonal multi-slice Turbo RARE T2-weighted images were acquired to render slice-positioning uniform (repetition time 2000 ms, echo time 15 ms, 16 slices of 0.4 mm). Field maps were acquired for each animal to assess field homogeneity, followed by local shimming, which corrects for the measured inhomogeneity in a rectangular volume within the brain.

Pharmacological MRI (PhMRI) procedures were performed using a single shot T2*-weighted echo planar imaging (EPI) sequence (repetition time 15000ms, echo time 25ms, 16 slices of 0.4 mm, 300 repetitions). The field-of-view was (20 x 20) mm² and the matrix size of (128 x 64), resulting in voxel dimensions of (0.156 x 0.312) mm². Baseline scans were acquired for 15 min (60 repetitions) after which a single bolus of medetomidine (0.3mg/kg) was administered through a subcutaneous (s.c.) catheter and the measurements continued until 60 min (240 repetitions) post-injection.

RsfMRI signals were measured by a single shot T2*-weighted EPI sequence (repetition time 2000 ms, echo time 15 ms, 16 slices of 0.4mm, 150 repetitions). The field-of-view was (20 x 20) mm² and the matrix size (128 x 64), resulting in voxel dimensions of (0.156 x 0.312) mm².

2.4. MRI data pre-processing

Preprocessing of the phMRI and pharmacological rsfMRI data, including realignment, normalization and smoothing, was performed using SPM8 software (Statistical Parametric Mapping, http://www.fil.ion.ucl.ac.uk) (Jonckers et al., 2011, Shah et al., 2013). First, all images within each session were realigned to the first image. This was done using a least squares approach and a 6-parameter (rigid body) spatial transformation. Second, all datasets were normalized to a study specific EPI template and coregistered to an anatomical T2 weighted template. The normalization steps consist of a global 12-parameter affine transformation followed by the estimation of the nonlinear deformations. Finally, in plane smoothing was done using a Gaussian kernel with full width at half maximum of twice the voxel size.

2.5. MRI data analysis

2.5.1: Pharmacological MRI

The data analysis for phMRI was performed in SPM8 (Statistical Parametric Mapping, http://www.fil.ion.ucl.ac.uk). For each animal the smoothed data were fitted to a generalized linear model (GLM) and the motion parameters resulting from the realignment were included as covariates to account for movement. For each animal the following conditions were evaluated: the first 15 min before medetomidine injection (60 baseline scans) versus 10 min, 20 min, 30 min, 40 min, 50 min and 60 min (each 40 scans) after the bolus injection. Mean difference images were computed in SPM8 for each condition using a whole brain mask and are shown on the anatomical template. Statistical analyses between conditions included a repeated-measures ANOVA and a post-hoc comparison was

made between baseline vs. 10, 20, 30, 40, 50 and 60 min post-injection (uncorrected, $p<0.001$, threshold of minimum 10 voxels).

2.5.1: Pharmacological rsfMRI: Independent Component Analysis

Considering the known effect of sedation on brain FC, it first had to be established whether the DMN-like network can be detected under medetomidine sedation. That is why a data-driven approach i.e. independent component analysis (ICA) was used to evaluate the existence of the DMN-like network under medetomidine sedation at 20 min and 50 min after the injection of the medetomidine bolus. ICA was performed for each group using the GIFT-toolbox (Group ICA of fMRI toolbox:http://icatb.sourceforge.net/), by implementing spatial ICA which estimates sources as being statistically spatially independent. First, a two-step data reduction step is performed by principal component analysis, after which the data of each individual animal is concatenated. Then group ICA is performed using the Infomax algorithm, which was successful at generating relevant neurological components in the mouse brain in previous studies (Jonckers et al., 2011). The final step is back reconstruction of the data to single-subject independent components and time courses. ICA was performed using a preset of 15 components, which was shown to be appropriate to identify the DMN-like network in mice (Sforazzini et al., 2014). Using the AMIRA software (Amira, Template Graphics Software, Inc., San Diego, California, USA), a template was created including the Default-Mode-like regions found in rodents (Lu et al., 2012) i.e. the prelimbic cortex, orbitofrontal cortex, cingulate cortex, retrosplenial cortex, parietal and temporal association cortex and hippocampus (**Online Resource ESM_1**). All neurologically relevant ICA components at 20 and 50 min post-injection are shown in **Online Resource ESM_2**. Using the GIFT-toolbox, spatial correlation (**Online Resource ESM_3**) was calculated between each of the 15 components per group and the DMN-template, to identify the DMN-like network component at 20 min and at 50 min after the medetomidine injection. The other ICA components were identified using the anatomical mouse brain atlas (Franklin and Paxinos, 1997) . For each ICA component a threshold was used so that only z-values above 1 were shown.

2.5.1: Pharmacological rsfMRI: seed-based analyses

All rsfMRI data were filtered between 0.01 and 0.1 Hz using the REST-toolbox (REST1.7, http://resting-fmri.sourceforge.net). Then, individual z-transformed FC-maps were obtained for all animals using a rectangular seed region of 8 voxels in the left cingulate cortex, orbitofrontal cortex, thalamus, caudate putamen, somatosensory cortex, motor cortex, visual cortex and nucleus accumbens (**Online Resource ESM_4**). The location of the seed regions was defined by selecting voxels with the highest z-score observed in the ICA maps. **Online Resource ESM_4** shows the location of the seed regions for each ICA component. In the seed-based analyses FC was calculated between the seed region and the remainder of the ICA component, which was included in a mask (**Online Resource ESM_4**). Statistical comparisons between groups and networks were performed using a one-way ANOVA and post-hoc comparisons were made comparing two groups (saline vs. pharmacological modulation or DMN-like network vs. other networks) with the Holms-Sidak correction for multiple comparisons.

For the seed-based analyses of the DMN-like network mean zFC-maps of the left cingulate cortex, which showed the highest z-score on the ICA map, were obtained for each group in SPM8 and are shown on the anatomical template. Comparison of the zFC-maps between groups was performed in SPM8 using a one-way ANOVA and a post-hoc comparison was made between saline vs. pharmacological modulation with the false discovery rate (FDR) correction for multiple comparisons ($p<0.05$, threshold of minimum 10 voxels).

3. Results

3.1. Acute cholinergic and serotonergic modulations

The effect of acute cholinergic and serotonergic inhibition on BOLD FC was evaluated for all the networks described in **Fig 1** i.e. the DMN-like network, orbitofrontal, thalamic, caudate putamen, somatosensory, motor, visual and nucleus accumbens network. The effects of acute cholinergic neurotransmission modulations on the DMN-like network (**Fig 1A**) in the mouse brain were evaluated with a seed-based analysis of the left cingulate cortex using the mAChR antagonist scopolamine. **Fig 2** shows that compared to the saline-treated group, scopolamine significantly decreased BOLD FC within the cingulate cortex (p-value=$1.36\text{x}10^{-3}$), with the retrosplenial cortex (p-value=$2.99\text{x}10^{-3}$), with

the orbitofrontal cortex (p-value=1.42x10^{-4}), with the temporal association cortex (p-value=4.94x10^{-3}) and with the parietal association cortex (p-value=8.35x10^{-5}).

The effects of acute serotonergic neurotransmission modulations on BOLD FC within the mouse DMN-like network were evaluated with a seed-based analysis of the left cingulate cortex using the 5HT1A antagonist WAY100135. **Fig 2** shows that compared to the saline-treated group, WAY100135 decreased BOLD FC within the cingulate cortex (p-value=1.54x10^{-3}), with the orbitofrontal cortex (p-value=1.89x10^{-5}), with the temporal association cortex (p-value=4.53x10^{-4}) and with the parietal association cortex (p-value=2.65x10^{-4}).

Additionally, the effects of cholinergic and serotonergic modulations were assessed for the other networks described in **Fig 1** i.e. the orbitofrontal (**Fig 1B**), thalamic (**Fig 1C**), caudate putamen (**Fig 1D**), somatosensory (**Fig 1E**), motor (**Fig 1F**), visual (**Fig 1G**) and nucleus accumbens network (**Fig 1H**). **Fig 2** shows that scopolamine significantly decreased BOLD FC within the orbitofrontal (p-value=1.52x10$^{\wedge-6}$), caudate putamen (p-value=8.25x10$^{\wedge-5}$), somatosensory (p-value=1.51x10$^{\wedge-4}$) and nucleus accumbens (p-value=5.80x10$^{\wedge-5}$) networks. WAY100135 significantly decreased BOLD FC within the orbitofrontal (p-value=6.84x10$^{\wedge-17}$), thalamic (p-value=3.56x10$^{\wedge-8}$), caudate putamen (p-value=5.35x10$^{\wedge-9}$), somatosensory (p-value=1.04x10$^{\wedge-3}$) and nucleus accumbens (p-value=2.20x10$^{\wedge-7}$) networks.

Online Resource ESM_5 shows that methyl-scopolamine, which has poor blood brain barrier permeability and therefore allows assessing the peripheral effect of scopolamine, does not affect any of the studied brain networks compared to saline-treated animals in terms of BOLD FC. Sumatriptan is an agonist of the 5HT1B/1D receptors, which are present specifically on the brain vessels, and causes cerebral vasoconstriction. **Online Resource ESM_5** shows that sumatriptan significantly decreased BOLD FC within the thalamic (p-value=4.83x10^{-4}) and somatosensory (p-value=7.83x10^{-3}) networks.

3.2. DMN-like network strength compared to other networks

Within each group, BOLD FC strength of the DMN-like network was compared to that of the orbitofrontal, thalamic, caudate putamen, somatosensory, motor, visual and nucleus accumbens networks. **Fig 3A** shows that in the saline-treated animals, BOLD FC within the DMN-like network was significantly stronger compared to the caudate putamen (p-value=1.67x10$^{\wedge-5}$), somatosensory (p-value=0.001), motor (p-value=0.001), visual (p-value=0.005) and nucleus accumbens (p-

value=4.12x10^{-8}) networks. BOLD FC of the DMN-like network was not significantly different compared to the orbitofrontal and thalamic networks. For the scopolamine-treated animals, BOLD FC of the DMN-like network was significantly stronger compared to the somatosensory (p-value=0.02) and nucleus accumbens (p-value=0.02) networks. For the WAY100135-treated group BOLD FC of the DMN-like network was significantly stronger compared to the orbitofrontal (p-value=2.61x10^{-7}), thalamic (p-value=3.00x10^{-4}), caudate putamen (p-value=1.89x10^{-5}) and nucleus accumbens (p-value=1.00x10^{-4}) networks.

Fig 3B shows that similar to the saline-treated group, BOLD FC of the DMN-like network in the methyl-scopolamine-treated animals was significantly stronger compared to the caudate putamen (p-value=4.70x10^{-3}), somatosensory (p-value=0.015), motor (p-value=7.50x10^{-4}), visual (p-value=1.29x10^{-5}) and nucleus accumbens (p-value=1.70x10^{-4}). The sumatriptan-treated group showed stronger BOLD FC of the DMN-like network compared to the thalamic (p-value=4.89x10^{-6}), caudate putamen (p-value=4.90x10^{-6}), somatosensory (p-value=3.23x10^{-7}), motor (p-value=1.90x10^{-4}), visual (p-value=2.73x10^{-5}) and nucleus accumbens (p-value=1.76x10^{-7}) networks.

3.3. The DMN-like network under medetomidine sedation

To ensure that the DMN-like network could be evaluated under medetomidine sedation, pharmacological MRI (phMRI) was performed to assess the T2* signal intensity changes over time induced by a single bolus of medetomidine (0.3mg/kg) (**Fig 4**). The results show that at 20 min post-injection medetomidine induced the most pronounced T2* signal intensity differences compared to baseline (p-value<0.0001). Moreover, these signal intensity differences decreased and stabilized from 30 min post-injection onwards.

RsfMRI was performed at 20 min and 50 min post-injection and analyzed with ICA. The time point of 20 min post-injection was chosen because the phMRI showed maximum T2* signal intensity changes. The time point of 50 min was chosen to ensure a minimum effect of medetomidine on T2* signal intensity. The DMN-like network component was identified by calculating the spatial correlation of each ICA component with a DMN-template. All relevant ICA components besides the DMN-like network observed at 20 min and 50 min post-injection are shown in **Online Resource ESM_2.** The spatial correlation values of each neurological ICA component with the DMN template at 20 min and 50 min post-injection are shown in **Online Resource ESM_3**. At 20 min post-injection the ICA component

with the highest spatial correlation with the DMN-template consisted of the prelimbic cortex, orbitofrontal cortex, cingulate cortex, retrosplenial cortex and parietal association cortex (**Fig 5A**, spatial correlation 0.4). At 50 min post-injection the ICA component with the highest spatial correlation with the DMN-template consisted the prelimbic cortex, orbitofrontal cortex, cingulate cortex, retrosplenial cortex, parietal association cortex, temporal association cortex, and the dentate gyrus, CA1 region and dorsal subiclum of the hippocampus (**Fig 5A,** spatial correlation 0.82). The ICA results show decreased BOLD FC of the DMN-like network with its posterior regions at 20 min post-injection, thus when medetomidine has its maximum effect in the brain, while at 50 min post-injection the entire DMN-like network could be observed.

Next, a seed-based analysis was performed with the left cingulate cortex as seed region (**Fig 5B**). The results confirm the ICA findings i.e. at 20 min post-injection the DMN-like network shows decreased BOLD FC with its posterior regions, i.e. the retrosplenial cortex and hippocampus regions, compared to 50 min post-injection (p-value=0.007), when the entire DMN-like network could be observed.

4.Discussion

The current study aimed to determine how acute modulations of the cholinergic and serotonergic system affect the DMN-like network and other functional networks in healthy mice using a rsfMRI approach. Because modulating neurotransmission implies that brain function is altered before the rsfMRI acquisition, the more suitable term 'pharmacological rsfMRI' was used.

Diminishing muscarinic cholinergic and serotonergic neurotransmission decreased FC in the healthy mouse DMN-like network. The mouse DMN-like network encompasses the prelimbic cortex, orbitofrontal cortex, cingulate cortex, retrosplenial cortex, parietal and temporal association cortex, and the dentate gyrus, CA1 region and dorsal subiculum of hippocampus. This finding is consistent with previous reports of the DMN-like network in healthy rats (Upadhyay et al., 2011, Lu et al., 2012) and mice (Sforazzini et al., 2014). Moreover, these results are supported by a recent study using functional and structural correlates to demonstrate the existence of a DMN-like network in mice that is for a large part similar to the human and monkey DMN (Stafford et al., 2014). The DMN-like network described by Sforazzini and colleagues also included the thalamus, which was to a lesser extent part of the DMN-like network component in the current study. We conjecture that the use of a different anesthetic

(medetomidine in this study versus halothane by Sforazzini and colleagues) might be a possible explanation for this discrepancy. Specific Default-Mode-like regions that were affected by cholinergic modulation included the cingulate, retrosplenial, orbitofrontal and parietal and temporal association cortices. This is consistent with the known overlap of mAChRs with many regions of the DMN (Levey et al., 1991). The involvement of the DMN in cognitive processes might be mediated through among others the mAChR, so disruptions of this receptor subtype might result in disruptions of DMN FC and cognitive functions, as occur in Alzheimer's disease (Sheline and Raichle, 2013). Consistent with that notion, a previous study shows how mAChR modulation results in FC deficits in Default-Mode-like key regions and that these FC deficits are related to cognitive disruptions (Shah et al., 2015). Moreover, functional MRI studies in human subjects showed that scopolamine induced altered activity (Sperling et al., 2002, Antonova et al., 2011) in DMN regions. Serotonergic modulation affected the cingulate, orbitofrontal and parietal and temporal association cortices which is consistent with studies in human subjects demonstrating the involvement of 5HT1A receptors in the regulation of the DMN (Hahn et al., 2012). The role of the DMN in memory processes and emotional behavior could be mediated through serotonergic receptors, deficits of which lead to DMN FC disruptions in e.g. depression and autism disorders (Sheline et al., 2009, Washington et al., 2014). Similar FC disruptions were induced in the DMN-like network by cholinergic and serotonergic modulations, with the exception of the additional involvement of the retrosplenial cortex after cholinergic modulation. Considering the similar changes elicited by both modulations it might be argued that the DMN-like network is not the appropriate network to discriminate disease processes affecting cholinergic and serotonergic receptors. It is however interesting to note that the retrosplenial cortex, which is the murine homologue of the human posterior cingulate cortex, is an important node that consistently shows FC deficits in Alzheimer's disease, which is characterized by cholinergic impairments. Nevertheless, this study shows that modulating both mAChR and 5HT1A receptors affects DMN-like network FC, suggesting that these receptor subtypes contribute to maintaining intact FC in the DMN-like network in healthy mice.

When investigating other brain networks besides the DMN-like network, it was observed that inhibiting the mAChRs significantly decreased FC within the orbitofrontal, caudate putamen, sensory and nucleus accumbens networks, consistent with the spatial extent of the mAChRs (Levey et al., 1991). These networks are involved in e.g. memory, motor control, sensory functions and motivated behavior, which are functions that can be attributed to the mAChRs (Mogenson et al., 1980, Jacobs et al., 1994,

Deiana et al., 2011, Nelson et al., 2014). Decreasing 5HT1A neurotransmission caused a very significant effect in the orbitofrontal network. The frontal cortex shows a very high density of 5HT receptors and is important for memory functions, emotional behavior, attention and introspective processing (Hahn et al., 2012). 5HT1A inhibition additionally decreased FC within the thalamic, caudate putamen, somatosensory and nucleus accumbens networks, consistent with the known involvement of serotonine in motor activity, sensory gating, and motivated behavior (Bishop et al., 2009, Clissold et al., 2013, van den Buuse, 2013). When comparing the effect of cholinergic and serotonergic modulation, the frontal and thalamic networks were more affected by the latter. This is consistent with observations in neurological disorders, such as depression and autism, characterized by frontal impairments and aberrant serotonergic functioning (Jeong et al., 2009, Albert et al., 2014).

Some neurotransmitter systems might be involved in regulating blood pressure and vascular tone directly in the brain or in the periphery due to expression of their receptors in the vasculature and outside the brain. The cholinergic system is involved in directly regulating vascular tone in the brain and in modulating cardiovascular function due to the presence of peripheral mAChR (Sato and Sato, 1995, Klinkenberg and Blokland, 2010). Scopolamine is a mAChR antagonist and causes peripheral and cerebral vasoconstriction, possibly partly causing the observed effects on FC in this study. Methyl-scopolamine, a scopolamine derivative that does not pass the blood-brain-barrier, was therefore included in this study. When methyl-scopolamine was administered in the same dose as scopolamine, no significant effect was observed on FC in any of the assessed brain networks, excluding the possibility that peripheral vasoconstriction might induce the observed FC changes. Besides peripheral effects, direct effects of pharmacological modulations on cerebral vasculature will also influence FC in the brain. Sumatriptan is a 5HT1B/D receptor agonist that is used in the treatment of migraine. These receptors are present on the cerebral vasculature and thus cause cerebral vasoconstriction. Since sumatriptan is administered systemically in this study peripheral vasoconstriction in the coronary arteries cannot be excluded. Nevertheless, the observed effects of sumatriptan on FC should be dominated by vascular changes. In this study, sumatriptan did not show significant FC changes in the DMN-like network. When assessing the other networks, the thalamic and sensory networks were significantly affected at the dose used in this study, suggesting that these networks are more prone to cerebrovascular changes in the brain.

An interesting observation is that DMN-like network functional connections are stronger than those within the caudate putamen, somatosensory, motor, visual and nucleus accumbens networks. A statistical comparison confirmed that the DMN-like network, frontal and thalamic network show stronger intra-network FC than the other assessed networks in saline-treated animals. This pattern of strong FC in the DMN-like network is still preserved to some extent after modulating the mAChR and 5HT1A receptors. On one hand this observation suggests that DMN-like network functional connections are stronger, consistent with the known importance of the DMN and its related functions, requiring it to be resilient. On the other hand, the DMN is affected in a wide array of mental disorders, suggesting it is a vulnerable network. Several studies demonstrated that brain regions with higher baseline neuronal activity are more prone to disease-induced changes (Bero et al., 2012, de Haan et al., 2012). This is consistent with the observation of stronger FC in the DMN-like network in this study and the fact that the DMN is affected in a wide array of neurological disorders. Of course, it has to be taken into account that the modulations performed in this study were acute and only one dose was used per modulation. Performing chronic modulations similar to pathological neurotransmission changes in diseases or using different dose ranges might provide more insight in the vulnerability or resilience of the DMN-like network.

A limitation of rsfMRI studies in mice is the required use of anesthetic agents. In this study the mice were sedated with medetomidine, an alfa-2-receptor agonist that is known to abolish functional connections in mice (Nasrallah et al., 2012, Nasrallah et al., 2014). The phMRI revealed major T2* signal intensity changes 20 min after the injection of the medetomidine bolus. At 30 min post-injection the effect of medetomidine on the brain decreased and stabilized. Similarly, the physiological data in this study showed that breathing rate and heart rate stabilized from 20-30 min post-injection onwards. The FC data showed that at 20 min post-injection i.e. when the effects of medetomidine peaked in the brain, the DMN-like network showed fronto-posterior disconnection between the cingulate and retrosplenial cortex/hippocampus regions, consistent with studies in human subjects where anesthesia affects cingulate-retrosplenial FC (Hudetz, 2012). This is also reflected by the observation of two ICA components showing a high spatial correlation with the DMN-template at 20 min-post-injection. The FC data showed that at 50 min post-injection the entire DMN-like network could be distinguished in one single ICA component. It has to be mentioned that the physiological parameters stabilized at 20-30 min after the medetomidine bolus injection in mice, so the observed FC deficits at 20 min vs. 50

min post-injection could be due to a higher level of physiological variability at 20 min post-injection. Starting from 30 min post-injection the effects of medetomidine on the T2* signal intensity values decrease and start to stabilize, resulting in more reliable FC networks compared to 20 min post-injection.

To conclude, this study shows that mAChR and 5HT1A receptors are important for the integrity of the DMN-like network in mice. The retrosplenial cortex was additionally affected by cholinergic modulation, consistent with studies in Alzheimer's disease where this region reliably shows FC deficits. Other networks are also affected, with the frontal and thalamic networks being disrupted to a greater extent by 5HT1A modulation. This is consistent with neurological disorders that are characterized by frontal impairments and aberrant serotonergic functioning, such as depression and autism disorders. Finally, the DMN-like network shows stronger FC compared to other brain networks in mice. Overall, this study demonstrates how rsfMRI can contribute to providing insight into the role of neurotransmitter systems in the integrity of functional networks in the healthy mouse brain. Moreover, this study shows how rsfMRI can contribute to discriminate the effect of modulating different neurotransmitter systems on functional networks, and paves the way to understanding the role of neurotransmitter systems in early-stage disease-induced functional network deficits.

Acknowledgements: This research was supported by the European Union's Seventh Framework Programme under grant agreement number 278850 (INMiND), by Molecular Imaging of Brain Pathophysiology (BRAINPATH) under grant agreement number 612360 within the Marie Curie Actions-Industry-Academia Partnerships and Pathways (IAPP) program, by Stichting Alzheimer Onderzoek (SAO-FRA) under grant agreement number 13026, by the Institute for the Promotion of Innovation by Science and Technology (IWT) in Flanders under grant agreement 131060, by the doctoral grant BOF-DOCPRO 2013 from the University of Antwerp and by Fonds Wetenschappelijk Onderzoek Vlaanderen (FWO) under grant agreement 1510514N. DS is holder of an IWT PhD grant. IB is holder of an FWO krediet aan navorser reasearch grant.

Figures

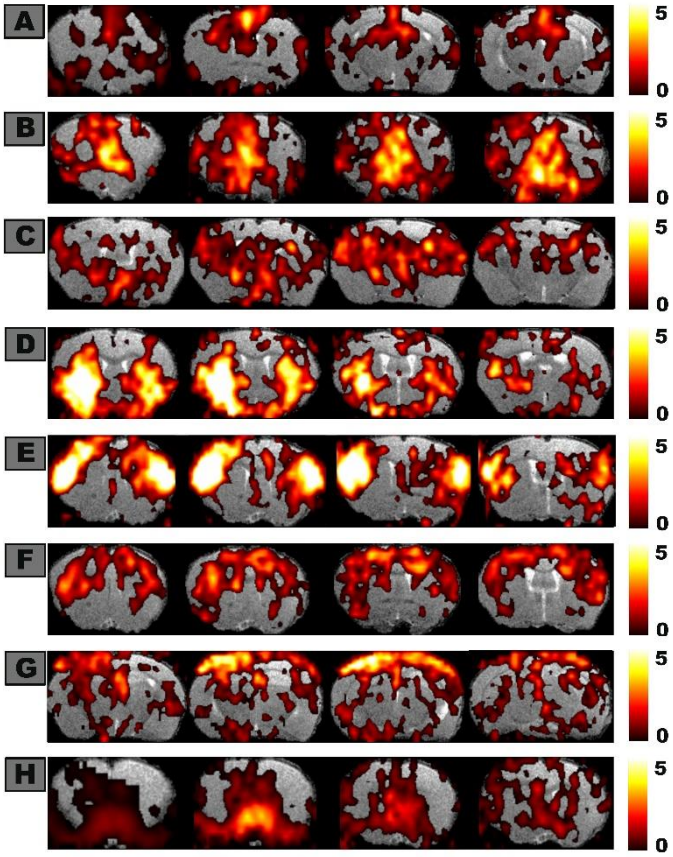

Fig 1: Relevant ICA components. This figure shows all neurological ICA components at 50 min post-injection. The color scale represents the z-value i.e. the strength of the BOLD functional correlation. The ICA components are shown on a T2-weighted anatomical MRI template. **A)** DMN-like network**, B)** orbitofrontal cortex, **C)** thalamus, **D)** caudate putamen, **E)** somatosensory cortex, **F)** motor cortex, **G)** visual cortex, **H)** nucleus accumbens.

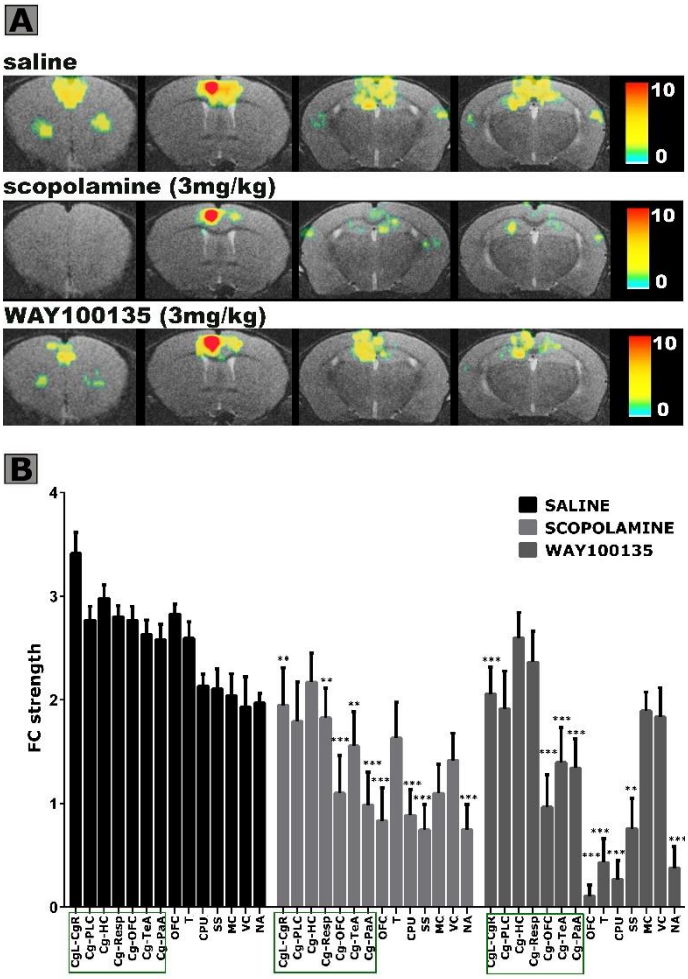

Fig 2: The effect of cholinergic and serotonergic inhibition on the DMN-like network and other networks. Panel A shows 4 consecutive slices of the mean statistical zFC-map of the left cingulate cortex. The mean statistical zFC-maps are shown for each group on a T2-weighted anatomical MRI template. The color scale represents the T-value i.e. the strength of the BOLD functional correlation with the left cingulate cortex. **Panel B** shows a graphical representation of mean BOLD FC strength ± SEM for the saline, scopolamine and WAY100135 group. Mean BOLD FC strength ± SEM are shown for each functional connection within the DMN-like network i.e. left cingulate cortex (CgL) with right cingulate cortex (CgR), prelimbic cortex (PLC), hippocampus (HC), retrosplenial cortex (Resp), orbitofrontal cortex (OFC), temporal association cortex (TeA) and parietal association cortex (PaA). The DMN-like network functional connections are indicated by the green box. Additionally, BOLD FC strength ± SEM was assessed within the orbitofrontal (OFC), thalamus (T), caudate putamen (Cpu), somatosensory (SS), motor (MC), visual (VC) and nucleus accumbens (NA) networks for each group. Statistical comparisons were made between saline vs. pharmacological modulation per network ** $p<0.01$, *** $p<0.001$.

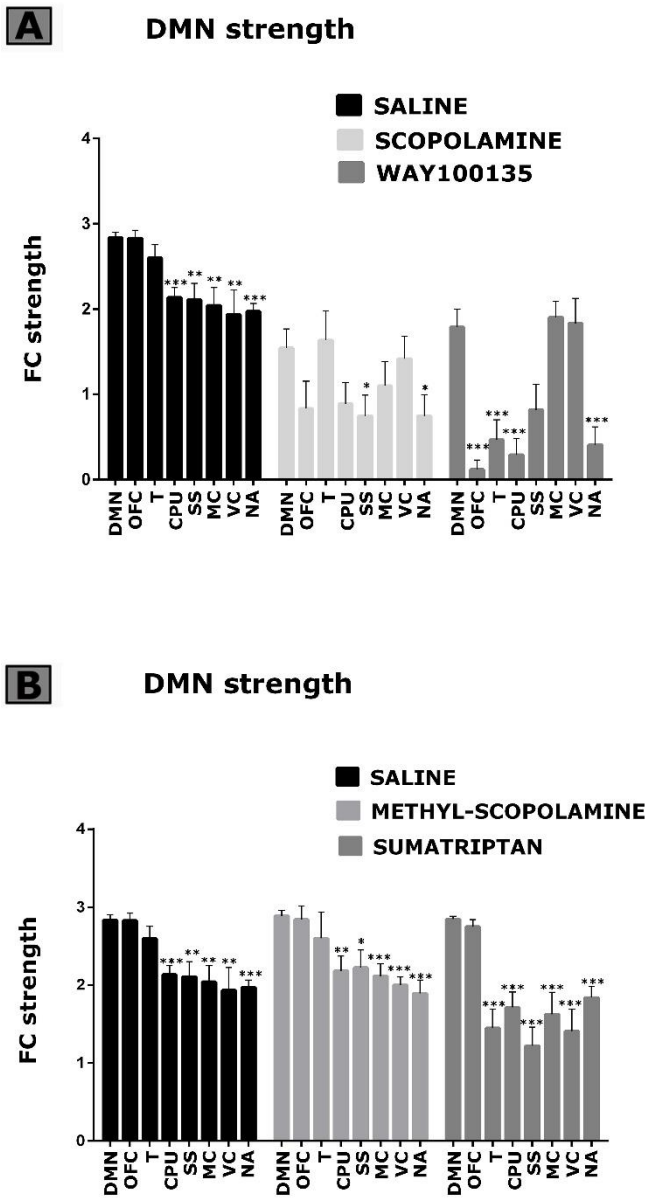

Fig 3: BOLD FC strength of the DMN-like network compared to other networks. This figure shows a graphical representation of mean BOLD FC strength ± SEM for the saline, scopolamine and WAY100135 group (**Panel A**) and saline, methyl-scopolamine and sumatriptan group (**Panel B**). BOLD FC strength ± SEM is shown for each functional connection within the DMN-like network, orbitofrontal (OFC), thalamus (T), caudate putamen (Cpu), somatosensory (SS), motor (MC), visual (VC) and nucleus accumbens (NA) networks. Statistical comparisons of BOLD FC strength were made within each group between DMN-like network vs. other networks ** $p<0.01$, *** $p<0.001$.

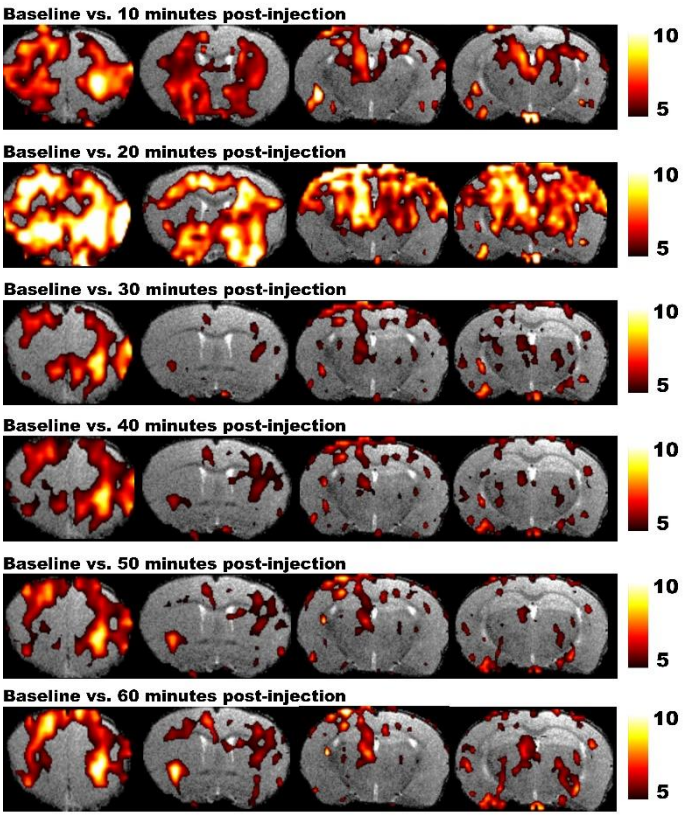

Fig 4: Results of phMRI with a single bolus of medetomidine. This figure shows 4 consecutive slices of the statistical difference maps of baseline vs. 10 min, 20 min, 30 min, 40 min, 50 min and 60 min post-injection. The statistical maps are shown on a T2-weighted anatomical MRI template. The color scale at the right indicates the T-value i.e. the strength of the T2* signal intensity difference induced by medetomidine vs. baseline in all conditions.

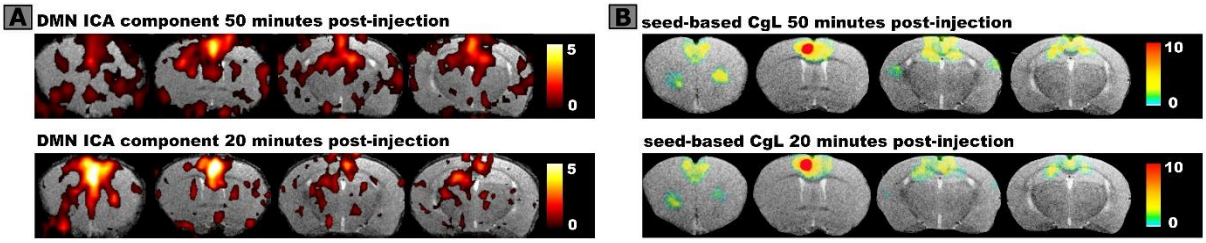

Fig 5: ICA and seed-based analysis of the DMN-like network at 20 min and 50 min after the medetomidine injection. Panel A shows 4 consecutive slices of the mean DMN-like network ICA component at 20 min and 50 min post-injection. The mean DMN-like network components are shown for each group on a T2-weighted anatomical MRI template. The color scale represents the z-value i.e. the strength of the BOLD functional correlation. **Panel B** shows 4 consecutive slices of the mean statistical zFC-map of the left cingulate cortex. The mean statistical zFC-maps are shown for each group on a T2-weighted anatomical MRI template. The color scale represents the T-value i.e. the strength of the BOLD functional correlation with the left cingulate cortex.

Supplementary Figures and Tables

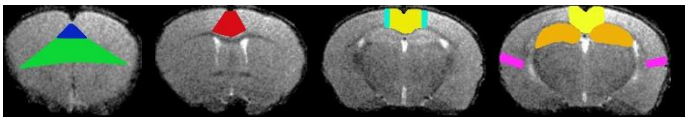

Online Resource ESM 1: Regions in the DMN-template. A spatial template was created containing the regions known to be part of the rodent DMN-like network i.e. the prelimbic cortex (blue), orbitofrontal cortex (green), cingulate cortex (red), retrosplenial cortex (yellow), hippocampus (dorsal subiculum, CA1 field and dentate gyrus) (orange), parietal association cortex (cyan), and temporal association cortex (fuchsia). The DMN-like network regions are shown on a T2-weighted anatomical MRI template.

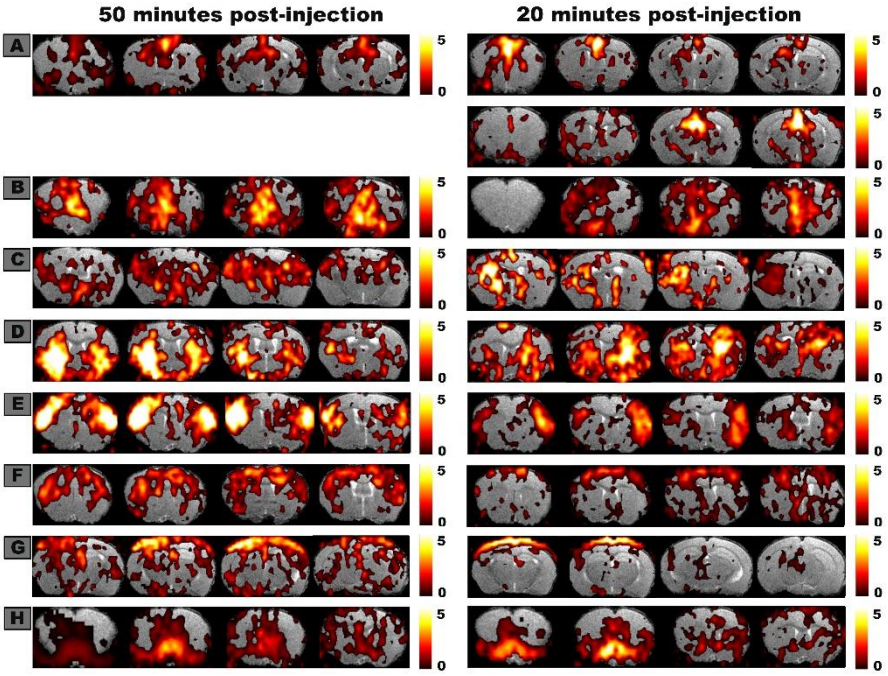

Online Resource ESM_2: **Relevant ICA components besides the DMN-like network at 20 min and 50 min after injection of the medetomidine bolus.** This figure shows all neurological ICA components besides the DMN-like network at 20 min and 50 min post-injection. The color scale represents the z-value i.e. the strength of the BOLD functional correlation. The ICA components are shown on a T2-weighted anatomical MRI template. **A)** DMN-like network**, B)** orbitofrontal cortex, **C)** thalamus, **D)** caudate putamen, **E)** somatosensory cortex, **F)** motor cortex, **G)** visual cortex, **H)** nucleus accumbens. At 20 min post-injection two components corresponded to the DMN-like network.

ICA-component	Spatial correlation with DMN template	
	20 min post-injection	50 min post-injection
Dentate gyrus/ CA1 region /dorsal subiculum hippocampus	0.37	/
Prelimbic ctx, orbitofrontal ctx, cingulate ctx, retrosplenial ctx, parietal association ctx, dentate gyrus/dorsal subiculum of the hippocampus, temporal association ctx	/	0.82
Prelimbic ctx, orbitofrontal ctx, cingulate ctx, retrosplenial ctx, parietal association ctx	0.40	/
Orbitofrontal ctx	0.1	0.09
Thalamus	0.13	0.17
Caudate putamen	0.08	0.08
Somatosensory ctx	0.04	0.07
Motor ctx	0.17	0.14
Visual ctx	0.08	0.11
Nucleus accumbens	0.09	0.07

Online Resource ESM 3: Spatial correlation of the 15 ICA components with the DMN template at 20 min and 50 min after the injection of medetomidine. This table shows the regions within each component and the spatial correlation value with the DMN-template at 20 min and 50 min post-injection. The components showing the highest spatial correlation with the DMN-template are indicated in blue. The component showing the second highest spatial correlation with the DMN-template at 20 min post-injection is shown in orange.

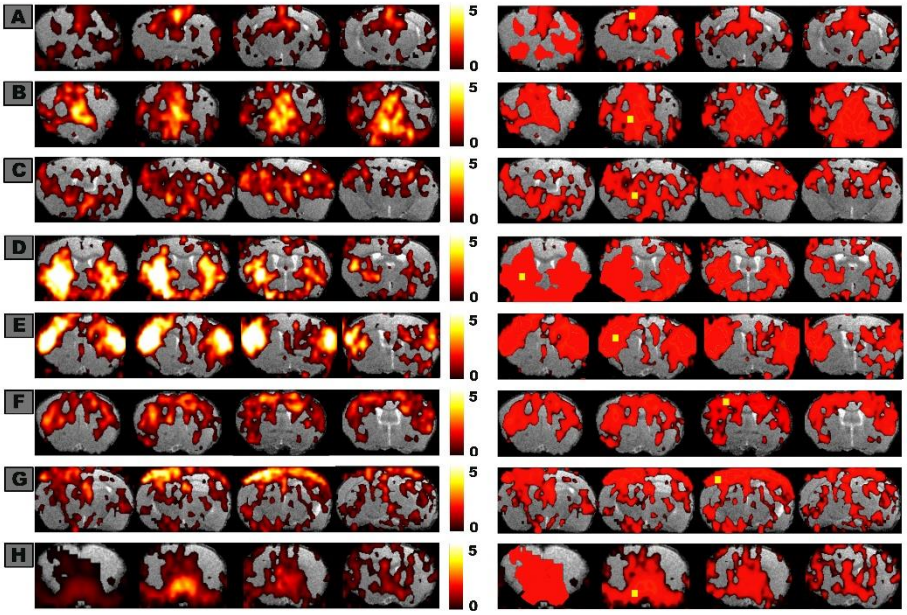

<u>Online Resource ESM_4:</u> Location of seed regions for seed-based analyses. This figure shows on the left all neurological ICA components at 50 min post-injection. The color scale represents the z-value i.e. the strength of the BOLD functional correlation. On the right the location of the seed-region (yellow) is shown for each ICA component, as well as the regions that were included in the mask for the seed-based analyses (red). The ICA components and regions for the seed-based analyses are shown on a T2-weighted anatomical MRI template. **A)** DMN-like network**, B)** orbitofrontal cortex, **C)** thalamus, **D)** caudate putamen, **E)** somatosensory cortex, **F)** motor cortex, **G)** visual cortex, **H)** nucleus accumbens.

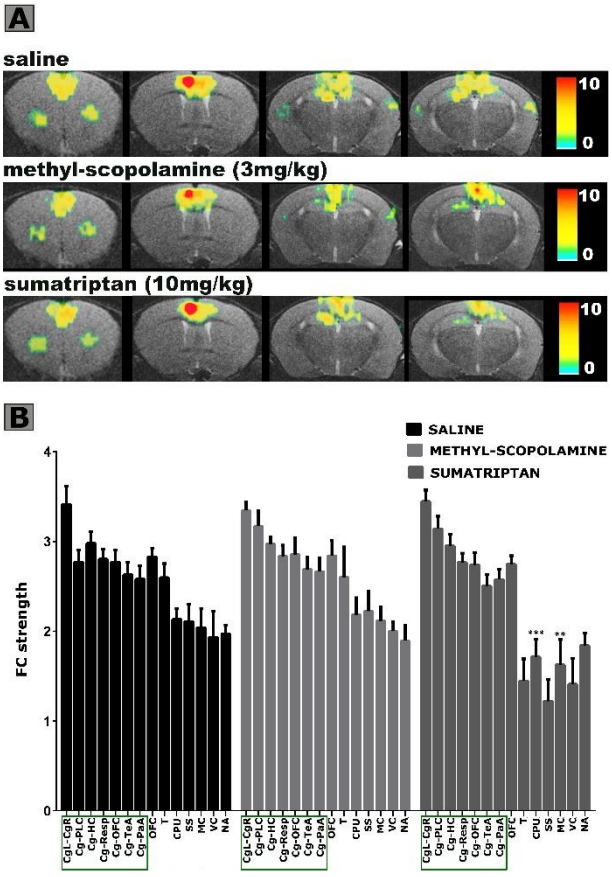

Online Resource ESM_5: The effect of peripheral and cerebral vasoconstriction on the DMN-like network and other networks. Panel A shows 4 consecutive slices of the mean statistical zFC-map of the left cingulate cortex. The mean statistical zFC-maps are shown for each group on a T2-weighted anatomical MRI template. The color scale represents the T-value i.e. the strength of the BOLD functional correlation with the left cingulate cortex. **Panel B** shows a graphical representation of mean BOLD FC strength ± SEM for the saline, methyl-scopolamine and sumatriptan group. Mean BOLD FC strength ± SEM are shown for each functional connection within the DMN-like network i.e. left cingulate cortex (CgL) with right cingulate cortex (CgR), prelimbic cortex (PLC), hippocampus (HC), retrosplenial cortex (Resp), orbitofrontal cortex (OFC), temporal association cortex (TeA) and parietal association cortex (PaA). The DMN-like network functional connections are indicated by the green box. Additionally, BOLD FC strength ± SEM was assessed within the orbitofrontal (OFC), thalamus (T), caudate putamen (Cpu), somatosensory (SS), motor (MC), visual (VC) and nucleus accumbens (NA) networks for each group. Statistical comparisons were made between saline vs. pharmacological modulation per network ** $p<0.01$, *** $p<0.001$.

Reference list

Albert PR, Vahid-Ansari F, Luckhart C (2014) Serotonin-prefrontal cortical circuitry in anxiety and depression phenotypes: pivotal role of pre- and post-synaptic 5-HT1A receptor expression. Frontiers in behavioral neuroscience 8:199.

Antonova E, Parslow D, Brammer M, Simmons A, Williams S, Dawson GR, Morris R (2011) Scopolamine disrupts hippocampal activity during allocentric spatial memory in humans: an fMRI study using a virtual reality analogue of the Morris Water Maze. Journal of psychopharmacology 25:1256-1265.

Bero AW, Bauer AQ, Stewart FR, White BR, Cirrito JR, Raichle ME, Culver JP, Holtzman DM (2012) Bidirectional relationship between functional connectivity and amyloid-beta deposition in mouse brain. The Journal of neuroscience : the official journal of the Society for Neuroscience 32:4334-4340.

Bishop C, Krolewski DM, Eskow KL, Barnum CJ, Dupre KB, Deak T, Walker PD (2009) Contribution of the striatum to the effects of 5-HT1A receptor stimulation in L-DOPA-treated hemiparkinsonian rats. Journal of neuroscience research 87:1645-1658.

Biswal B, Yetkin FZ, Haughton VM, Hyde JS (1995) Functional connectivity in the motor cortex of resting human brain using echo-planar MRI. Magnetic resonance in medicine : official journal of the Society of Magnetic Resonance in Medicine / Society of Magnetic Resonance in Medicine 34:537-541.

Brier MR, Thomas JB, Ances BM (2014) Network dysfunction in Alzheimer's disease: refining the disconnection hypothesis. Brain connectivity 4:299-311.

Broyd SJ, Demanuele C, Debener S, Helps SK, James CJ, Sonuga-Barke EJ (2009) Default-mode brain dysfunction in mental disorders: a systematic review. Neuroscience and biobehavioral reviews 33:279-296.

Buckner RL, Andrews-Hanna JR, Schacter DL (2008) The brain's default network: anatomy, function, and relevance to disease. Annals of the New York Academy of Sciences 1124:1-38.

Buckner RL, Sepulcre J, Talukdar T, Krienen FM, Liu H, Hedden T, Andrews-Hanna JR, Sperling RA, Johnson KA (2009) Cortical hubs revealed by intrinsic functional connectivity: mapping, assessment of stability, and relation to Alzheimer's disease. The Journal of neuroscience : the official journal of the Society for Neuroscience 29:1860-1873.

Bullmore E, Sporns O (2009) Complex brain networks: graph theoretical analysis of structural and functional systems. Nature reviews Neuroscience 10:186-198.

Carli M, Balducci C, Samanin R (2000) Low doses of 8-OH-DPAT prevent the impairment of spatial learning caused by intrahippocampal scopolamine through 5-HT(1A) receptors in the dorsal raphe. British journal of pharmacology 131:375-381.

Carli M, Luschi R, Garofalo P, Samanin R (1995a) 8-OH-DPAT impairs spatial but not visual learning in a water maze by stimulating 5-HT1A receptors in the hippocampus. Behavioural brain research 67:67-74.

Carli M, Luschi R, Samanin R (1995b) (S)-WAY 100135, a 5-HT1A receptor antagonist, prevents the impairment of spatial learning caused by intrahippocampal scopolamine. European journal of pharmacology 283:133-139.

Clissold KA, Choi E, Pratt WE (2013) Serotonin 1A, 1B, and 7 receptors of the rat medial nucleus accumbens differentially regulate feeding, water intake, and locomotor activity. Pharmacology, biochemistry, and behavior 112:96-103.

Damoiseaux JS, Rombouts SA, Barkhof F, Scheltens P, Stam CJ, Smith SM, Beckmann CF (2006) Consistent resting-state networks across healthy subjects. Proceedings of the National Academy of Sciences of the United States of America 103:13848-13853.

de Haan W, Mott K, van Straaten EC, Scheltens P, Stam CJ (2012) Activity dependent degeneration explains hub vulnerability in Alzheimer's disease. PLoS computational biology 8:e1002582.

Deiana S, Platt B, Riedel G (2011) The cholinergic system and spatial learning. Behavioural brain research 221:389-411.

Dorr A, Sled JG, Kabani N (2007) Three-dimensional cerebral vasculature of the CBA mouse brain: a magnetic resonance imaging and micro computed tomography study. NeuroImage 35:1409-1423.

File SE, Gonzalez LE, Andrews N (1996) Comparative study of pre- and postsynaptic 5-HT1A receptor modulation of anxiety in two ethological animal tests. The Journal of neuroscience : the official journal of the Society for Neuroscience 16:4810-4815.

Fleming SM, Weil RS, Nagy Z, Dolan RJ, Rees G (2010) Relating introspective accuracy to individual differences in brain structure. Science 329:1541-1543.

Fletcher A, Bill DJ, Bill SJ, Cliffe IA, Dover GM, Forster EA, Haskins JT, Jones D, Mansell HL, Reilly Y (1993) WAY100135: a novel, selective antagonist at presynaptic and postsynaptic 5-HT1A receptors. European journal of pharmacology 237:283-291.

Franklin K, Paxinos G (1997) The Mouse Brain in Stereotaxic Coordinates. Third edition. Academic Press, San Diego.

Ghelardini C, Galeotti N, Figini M, Imperato A, Nicolodi M, Sicuteri F, Gessa GL, Bartolini A (1996) The central cholinergic system has a role in the antinociception induced in rodents and guinea pigs by the antimigraine drug sumatriptan. The Journal of pharmacology and experimental therapeutics 279:884-890.

Ghelardini C, Galeotti N, Vivoli E, Grazioli I, Uslenghi C (2009) The central analgesia induced by antimigraine drugs is independent from Gi proteins: superiority of a fixed combination of indomethacin, prochlorperazine and caffeine, compared to sumatriptan, in an in vivo model. The journal of headache and pain 10:435-440.

Hahn A, Wadsak W, Windischberger C, Baldinger P, Hoflich AS, Losak J, Nics L, Philippe C, Kranz GS, Kraus C, Mitterhauser M, Karanikas G, Kasper S, Lanzenberger R (2012) Differential modulation of the default mode network via serotonin-1A receptors. Proceedings of the National Academy of Sciences of the United States of America 109:2619-2624.

Hannawi Y, Lindquist MA, Caffo BS, Sair HI, Stevens RD (2015) Resting brain activity in disorders of consciousness: A systematic review and meta-analysis. Neurology 84:1272-1280.

Hudetz AG (2012) General anesthesia and human brain connectivity. Brain connectivity 2:291-302.
Iwabuchi SJ, Krishnadas R, Li C, Auer DP, Radua J, Palaniyappan L (2015) Localized connectivity in depression: A meta-analysis of resting state functional imaging studies. Neuroscience and biobehavioral reviews 51:77-86.
Jacobs SE, Fine A, Juliano SL (1994) Cholinergic basal forebrain transplants restore diminished metabolic activity in the somatosensory cortex of rats with acetylcholine depletion. The Journal of neuroscience : the official journal of the Society for Neuroscience 14:697-711.
Jeong B, Wible CG, Hashimoto R, Kubicki M (2009) Functional and anatomical connectivity abnormalities in left inferior frontal gyrus in schizophrenia. Human brain mapping 30:4138-4151.
Jonckers E, Van Audekerke J, De Visscher G, Van der Linden A, Verhoye M (2011) Functional connectivity fMRI of the rodent brain: comparison of functional connectivity networks in rat and mouse. PloS one 6:e18876.
Klinkenberg I, Blokland A (2010) The validity of scopolamine as a pharmacological model for cognitive impairment: a review of animal behavioral studies. Neuroscience and biobehavioral reviews 34:1307-1350.
Lee MH, Smyser CD, Shimony JS (2013) Resting-state fMRI: a review of methods and clinical applications. AJNR American journal of neuroradiology 34:1866-1872.
Levey AI, Kitt CA, Simonds WF, Price DL, Brann MR (1991) Identification and localization of muscarinic acetylcholine receptor proteins in brain with subtype-specific antibodies. The Journal of neuroscience : the official journal of the Society for Neuroscience 11:3218-3226.
Lu H, Zou Q, Gu H, Raichle ME, Stein EA, Yang Y (2012) Rat brains also have a default mode network. Proceedings of the National Academy of Sciences of the United States of America 109:3979-3984.
Mogenson GJ, Jones DL, Yim CY (1980) From motivation to action: functional interface between the limbic system and the motor system. Progress in neurobiology 14:69-97.
Monk CS, Peltier SJ, Wiggins JL, Weng SJ, Carrasco M, Risi S, Lord C (2009) Abnormalities of intrinsic functional connectivity in autism spectrum disorders. NeuroImage 47:764-772.
Nasrallah FA, Low SM, Lew SK, Chen K, Chuang KH (2014) Pharmacological insight into neurotransmission origins of resting-state functional connectivity: alpha2-adrenergic agonist vs antagonist. NeuroImage 103:364-373.
Nasrallah FA, Tan J, Chuang KH (2012) Pharmacological modulation of functional connectivity: alpha2-adrenergic receptor agonist alters synchrony but not neural activation. NeuroImage 60:436-446.
Nelson AB, Hammack N, Yang CF, Shah NM, Seal RP, Kreitzer AC (2014) Striatal cholinergic interneurons Drive GABA release from dopamine terminals. Neuron 82:63-70.
Przegalinski E, Tatarczynska E, Chojnacka-Wojcik E (1995) The role of hippocampal 5-hydroxytryptamine 1A (5-HT1A) receptors in the anticonflict activity of beta-adrenoceptor antagonists. Neuropharmacology 34:1211-1217.

Roberts AC (2011) The importance of serotonin for orbitofrontal function. Biological psychiatry 69:1185-1191.

Rohrer JD, Rosen HJ (2013) Neuroimaging in frontotemporal dementia. International review of psychiatry 25:221-229.

Salvador R, Sarro S, Gomar JJ, Ortiz-Gil J, Vila F, Capdevila A, Bullmore E, McKenna PJ, Pomarol-Clotet E (2010) Overall brain connectivity maps show cortico-subcortical abnormalities in schizophrenia. Human brain mapping 31:2003-2014.

Sato A, Sato Y (1995) Cholinergic neural regulation of regional cerebral blood flow. Alzheimer disease and associated disorders 9:28-38.

Schwarz RD, Callahan MJ, Coughenour LL, Dickerson MR, Kinsora JJ, Lipinski WJ, Raby CA, Spencer CJ, Tecle H (1999) Milameline (CI-979/RU35926): a muscarinic receptor agonist with cognition-activating properties: biochemical and in vivo characterization. The Journal of pharmacology and experimental therapeutics 291:812-822.

Sforazzini F, Schwarz AJ, Galbusera A, Bifone A, Gozzi A (2014) Distributed BOLD and CBV-weighted resting-state networks in the mouse brain. NeuroImage 87:403-415.

Shah D, Blockx I, Guns PJ, De Deyn PP, Van Dam D, Jonckers E, Delgado YPR, Verhoye M, Van der Linden A (2015) Acute modulation of the cholinergic system in the mouse brain detected by pharmacological resting-state functional MRI. NeuroImage 109:151-159.

Shah D, Jonckers E, Praet J, Vanhoutte G, Delgado YPR, Bigot C, D'Souza DV, Verhoye M, Van der Linden A (2013) Resting state FMRI reveals diminished functional connectivity in a mouse model of amyloidosis. PloS one 8:e84241.

Sheline YI, Barch DM, Price JL, Rundle MM, Vaishnavi SN, Snyder AZ, Mintun MA, Wang S, Coalson RS, Raichle ME (2009) The default mode network and self-referential processes in depression. Proceedings of the National Academy of Sciences of the United States of America 106:1942-1947.

Sheline YI, Raichle ME (2013) Resting state functional connectivity in preclinical Alzheimer's disease. Biological psychiatry 74:340-347.

Sperling R, Greve D, Dale A, Killiany R, Holmes J, Rosas HD, Cocchiarella A, Firth P, Rosen B, Lake S, Lange N, Routledge C, Albert M (2002) Functional MRI detection of pharmacologically induced memory impairment. Proceedings of the National Academy of Sciences of the United States of America 99:455-460.

Stafford JM, Jarrett BR, Miranda-Dominguez O, Mills BD, Cain N, Mihalas S, Lahvis GP, Lattal KM, Mitchell SH, David SV, Fryer JD, Nigg JT, Fair DA (2014) Large-scale topology and the default mode network in the mouse connectome. Proceedings of the National Academy of Sciences of the United States of America 111:18745-18750.

Upadhyay J, Baker SJ, Chandran P, Miller L, Lee Y, Marek GJ, Sakoglu U, Chin CL, Luo F, Fox GB, Day M (2011) DMN-like network activation in awake rodents. PloS one 6:e27839.

van den Buuse M (2013) Exploring the role of 5-HT1A receptors in the regulation of prepulse inhibition in mice: implications for cross-species comparisons. ACS chemical neuroscience 4:149-160.

Veer IM, Beckmann CF, van Tol MJ, Ferrarini L, Milles J, Veltman DJ, Aleman A, van Buchem MA, van der Wee NJ, Rombouts SA (2010) Whole brain resting-state analysis reveals decreased functional connectivity in major depression. Frontiers in systems neuroscience 4.

Washington SD, Gordon EM, Brar J, Warburton S, Sawyer AT, Wolfe A, Mease-Ference ER, Girton L, Hailu A, Mbwana J, Gaillard WD, Kalbfleisch ML, VanMeter JW (2014) Dysmaturation of the default mode network in autism. Human brain mapping 35:1284-1296.

Yu H, Lewander T (1997) Pharmacokinetic and pharmacodynamic studies of (R)-8-hydroxy-2-(di-n-propylamino)tetralin in the rat. European neuropsychopharmacology : the journal of the European College of Neuropsychopharmacology 7:165-172.